PERGAMON

Journal of Structural Geology 22 (2000) 1221–1231

JOURNAL OF STRUCTURAL GEOLOGY

www.elsevier.nl/locate/jstrugeo

Fracture dimensions, displacements and fluid transport

Agust Gudmundsson

Geological Institute, University of Bergen, Allegaten 41, N-5007 Bergen, Norway

Received 10 March 1999; accepted 26 April 2000

Abstract

There is commonly a linear relationship between the lengths of rock fractures and their displacements, but for many fracture populations there is a very large scatter in the data. In the lava flows of the rift zone in Iceland, the displacements on a fracture or fault of a given length may vary by a factor of 2–10. Similar scatter is obtained for the aperture (width)/length ratios of several hundred mineral-filled veins in a major fault zone. I propose that the displacement on a fracture depends mostly on the smaller of its dip and strike dimensions, referred to as the controlling dimension. Thus, in a horizontal outcrop, fractures with the same strike dimension (outcrop length) can have widely different displacements depending on whether the displacements of individual fractures are controlled by strike or dip dimensions. During growth of a fracture, its controlling dimension may alternate between the dip dimension and the strike dimension. The volumetric rate of flow of fluid through a rock fracture with smooth, parallel walls depends on the cube of the fracture aperture. This cubic law implies that when the aperture of a fracture of a given length in a single set or population can vary by a factor of 2–10, the corresponding volumetric rate of fluid flow through that fracture can vary by a factor of 8–1000. A single, wide fracture in a set of as many as several hundred fractures may thus largely dominate the fluid transport through that set. Fracture aperture depends not only on the associated stress field, but also on its controlling dimension.

1. Introduction

Fracture populations formed in a single tectonic regime with essentially uniform mechanical host-rock properties (Figs. 1 and 2) commonly show an approximately linear relationship between surface length and maximum displacement (Cowie and Scholz, 1992; Gudmundsson, 1992; Dawers et al., 1993; Cartwright et al., 1995; Clark and Cox, 1996; Marrett, 1996; Schlische et al., 1996; Schultz, 1997). There is, however, normally a very large scatter in the data (Cowie et al., 1996); not only when different sets are grouped together, but also when individual sets are considered (Figs. 3 and 4). Part of this scatter is, of course, attributable to the 'noise' that is invariably associated with empirical data.

For rock fractures, this noise is partly due to inaccurate measurements of displacement, and partly due to the concept of 'fracture length' being based on an operational definition which is neither very precise nor necessarily the same for all workers. For example, Gudmundsson (1987a,b) defines fracture length for fissure swarms in the rift zone of Iceland as the distance that a fracture can be traced on aerial photographs at the scale of around 1:30,000. All small fractures, whether or not they are associated with large fractures, are then regarded as separate fractures. The length distribution of a fracture population measured in this way is clearly subject to a truncation bias, because of inability to recognise fractures shorter than a certain threshold length. Other workers use different ways to determine fracture length; some of these are discussed by Odling (1997). Also, closely spaced, collinear cracks may act mechanically as single fractures (e.g. Sneddon and Lowengrub, 1969), and their interaction affects the measured length/width (aperture) ratios (Pollard et al., 1982; Gudmunds-

E-mail address: agust.gudmundsson@geol.uib.no (A. Gudmundsson).

0191-8141/00/$ - see front matter
PII: S0191-8141(00)00052-3

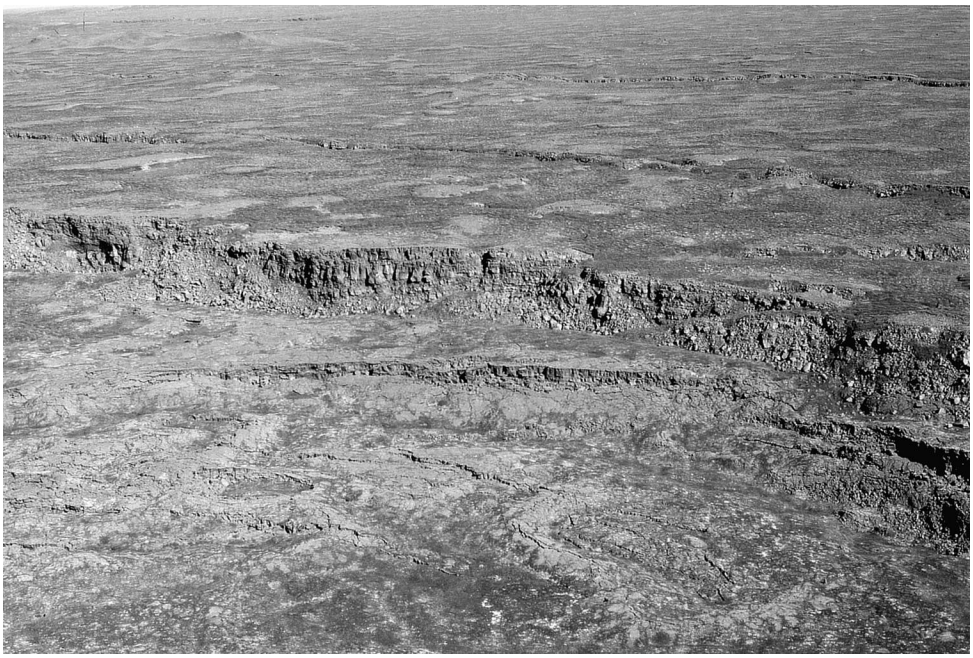

Fig. 1. Aerial view of some of the 144 tension fractures (lower half of the photograph) measured and plotted in Fig. 3. View northeast, the fractures are located in an early Holocene pahoehoe (basaltic) lava flow of the Theistareykir Fissure Swarm in the rift zone of North Iceland (cf. Gudmundsson, 1995, 1999). All the measured tension fractures occur in the region to the west of the main normal fault (maximum vertical displacement 24 m to the west).

Fig. 2. Western part of the Thingvellir Fissure Swarm in Southwest Iceland (cf. Gudmundsson, 1987b) where part of the data measured and plotted in Fig. 4 were obtained. The fissure swarm is located in an early Holocene pahoehoe (basaltic) lava flow. View southwest along part of the western boundary fault, Almannagja. The maximum vertical displacement on the fault occurs near the large house (a hotel) close to the lake and is around 40 m, whereas the width (opening) is mostly between 40 m and 60 m in the part of the fault used as channel by the river. There are pure extension (tension) fractures to the left of the main fault, many a few hundred metres long, some of which are filled with groundwater; the partly visible fracture at the left margin of the photograph is the one in Fig. 9. Houses and cars inside the graben provide a scale.

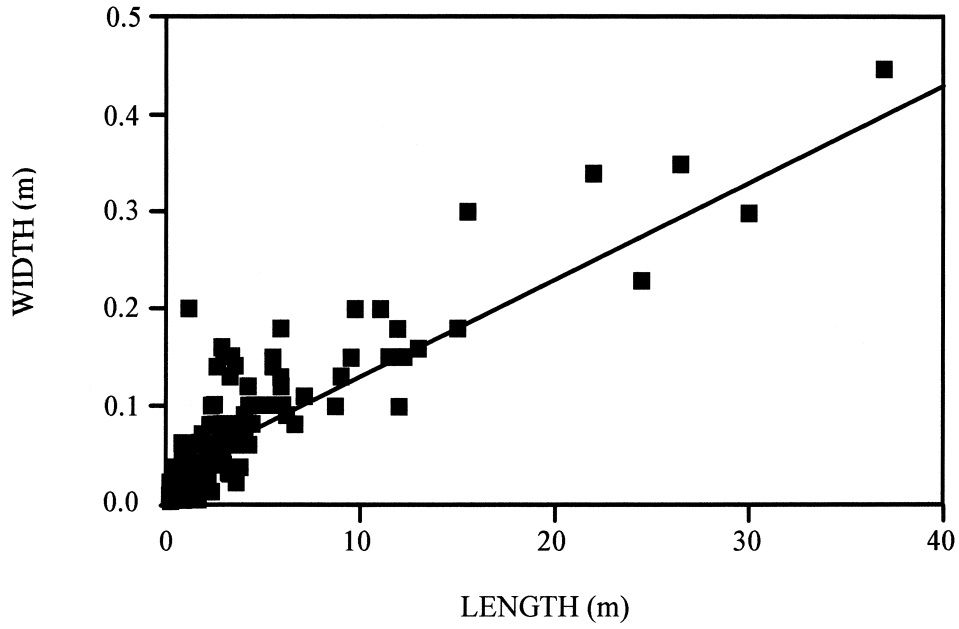

Fig. 3. Length–width (opening) relationship for 144 extension (mode I) fractures in a pahoehoe Holocene lava flow of the Theistareykir Fissure Swarm in the rift zone in North Iceland (cf. Fig. 1). All the fractures are measured within a single lava flow in an area of less than 0.1 km^2. There is a large scatter in the data: for some fractures of the same length, the width varies by a factor as great as 5–10. The most common variation, however, is by a factor of 2–3.

son, 1987a; Vermilye and Scholz, 1995; Willemse et al., 1996). In this paper the definition of fracture length follows that given by Gudmundsson (1987a,b).

Commonly, the scatter for a single fracture data set, measured by a single worker in a single tectonic regime, is so large that it can hardly be accounted for as noise. For example, in the data sets in Figs. 3 and 4

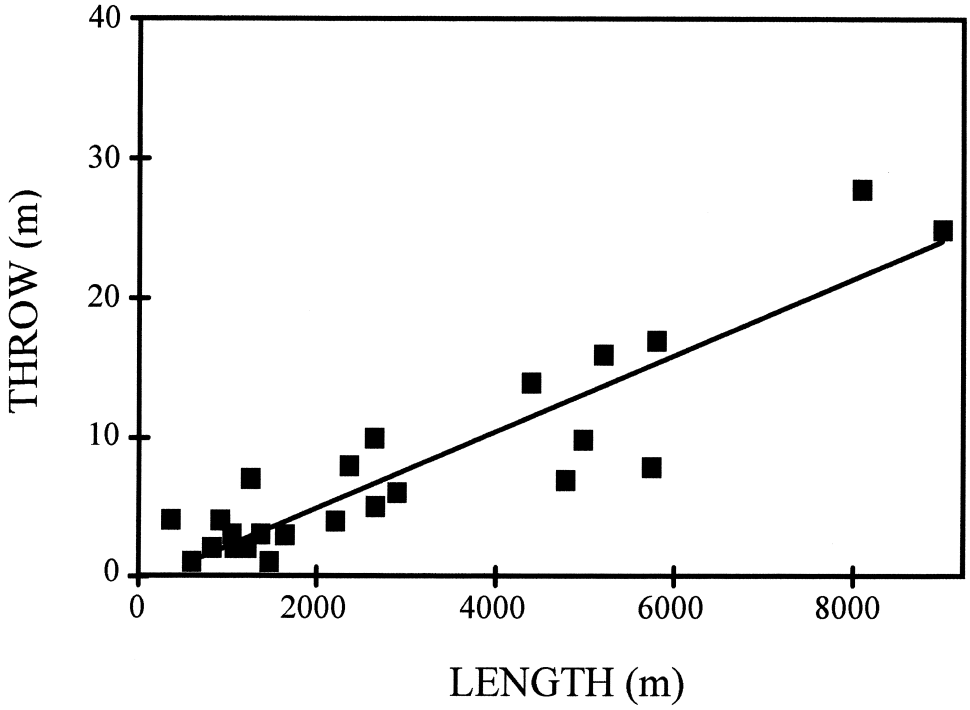

Fig. 4. Length–vertical displacement (throw) relationship for 26 large normal faults in the rift zone of Southwest Iceland (data from Gudmundsson, 1992). All the faults are from early Holocene pahoehoe lava flows with essentially the same mechanical properties (cf. Fig. 2). There is a considerable scatter in the data; for faults with lengths of roughly 6 km the throw can vary from about 8 m to 16 m, a factor of 2.

the displacements for a fracture of a given length vary by a factor of 2–10. Such a large scatter is likely to be significant and related to the mechanics of fracture initiation and development.

The way by which the width or aperture of a fracture changes with its dimensions has particularly important implications for fluid flow through the fracture. This follows because the volumetric flow rate through an isolated fracture with smooth, parallel fracture walls is proportional to the cube of the aperture of the fracture. However, this relationship does not hold for fractures with rough walls, or where the fracture aperture varies much along the trace of the fracture, in which case channelling of the fluid flow along the widest parts of the fracture may be important (Tsang and Neretnieks, 1998).

In the geological literature, fractures that reach the surface of the body within which they occur, or meet with other fractures or discontinuities, are referred to as restricted, whereas interior cracks are referred to as non-restricted (Nicol et al., 1996). In networks, where the cracks are commonly restricted and their controlling dimensions subject to temporal and spatial changes during the evolution of the network, the relationships between aperture and length are different from those of isolated, non-restricted cracks (Lee and Farmer, 1993; Odling, 1997). For understanding fluid flow in rock fractures, the crack dimensions and their effects on fracture displacements or openings must be considered.

One objective of this paper is to demonstrate the effect that controlling dimensions of fractures have on their displacements and, thereby, on the length–displacement relations and scatter for fracture sets. The paper presents some general equations for calculating fracture displacements when the boundary conditions, the elastic properties of the host rock, and the controlling dimensions for the fractures are known. A second objective is to discuss the implications of fracture dimensions and displacements or apertures for fluid flow in rock fractures.

2. Controlling dimensions

In fracture mechanics, there are three basic types of displacements of the crack surfaces (e.g. Broberg, 1999). In mode I displacement, referred to as opening or tensile mode, the crack surfaces move directly apart. In mode II displacement, referred to as sliding or in-plane shear mode, the fracture surfaces slide over one another in a direction perpendicular to the leading edge (tip) of the crack. In mode III displacement, referred to as tearing or anti-plane shear mode, the crack surfaces move relative to one another in a direction that is parallel to the leading edge (tip) of the crack.

For modelling an extension fracture, such as a pure tension fracture, or a hydrofracture such as a mineral vein or a dyke, the appropriate model is a mode I crack. For a large strike-slip fault, the appropriate model is normally a mode III crack. For a dip-slip fault, however, either a mode II crack or a mode III crack may be an appropriate model, depending on the controlling dimension of the fault. Furthermore, the controlling dimension depends on the shape of the fracture.

There are three basic ideal shapes that elliptical fractures can have (Fig. 5). First, a through-the-thickness crack (a through crack) goes right through the elastic body which contains the crack. Second, a thumbnail crack (a part-through crack) goes only partly into the elastic body from its surface. Third, an elliptical interior crack (of which the circular 'penny-shaped' crack is a special case) is located in the interior of the elastic body, which is then regarded as infinite. For two-dimensional cracks, one dimension, say the strike dimension of a large strike-slip fault, is effectively taken as infinite, in which case the other dimension (the dip in this case) must control the slip. To demonstrate that the smaller dimension is normally the one that largely or wholly controls fracture slip, we consider a three-dimensional elliptical crack (Fig. 5).

The problem of an elliptical crack in an infinite elastic solid subject to mode I (opening mode) loading was solved by Green and Sneddon (1950) and for arbitrary (mixed-mode) loading by Kassir and Sih (1966). A summary and a further discussion of these solutions is given by Sih and Liebowitz (1968) and by Kassir and Sih (1975). The controlling dimension of a three-dimensional crack subject to mode I loading can be represented by easily understood analytical formulas and is examined here.

Consider an elliptical crack with a tip-line described by the formula for an ellipse with the origin at the centre of the co-ordinate system and the major axis, $2a$, coinciding with the x-axis (and the minor axis, $2b$, coinciding with the y-axis), namely:

$$1 - \frac{x^2}{a^2} - \frac{y^2}{b^2} = 0 \tag{1}$$

where $a \geq b > 0$ (Fig. 5). The eccentricity of the ellipse, ε, is defined by:

$$\varepsilon = \left(1 - \frac{b^2}{a^2}\right)^{1/2} \tag{2}$$

where $0 < \varepsilon < 1$. The normal displacement, which is half the aperture, Δu_I, of the elliptical crack, as a function of location on the crack surface, $u = u(x,y,0)$, is

given by:

$$u = \frac{-\sigma(1-\nu)b}{GE(\varepsilon)}\left(1 - \frac{x^2}{a^2} - \frac{y^2}{b^2}\right)^{1/2} \quad (3)$$

where $-\sigma$ is the tensile stress opening the crack (considered negative), ν is Poisson's ratio of the host rock, G its shear modulus, and $E(\varepsilon)$ is the complete elliptic integral of the second kind, defined by:

$$E(\varepsilon) = \int_0^{\pi/2} \sqrt{1 - \varepsilon^2 \sin^2\theta}\, \mathrm{d}\theta. \quad (4)$$

This integral cannot be evaluated by elementary techniques for general values of ε; standard mathematical tables, however, give $E(\varepsilon)$ for various values of ε (Beyer, 1976).

Consider first a circular interior crack, a penny-shaped crack, where, by definition, $a = b$. Then from Eq. (2) we have $\varepsilon = 0$, and from Beyer (1976, p. 464), $E(0) = \pi/2 \cong 1.57$. Using $a = b$, and the relations $x^2 + y^2 = r^2$ (where r is the radial co-ordinate of a circle with its centre at the origin) and $G = E/[2(1+\nu)]$, where E is Young's modulus, from Eq. (3) the normal displacement $u = u(r)$ is:

$$u = \frac{-4\sigma(1-\nu^2)}{\pi E}(b^2 - r^2)^{1/2}. \quad (5)$$

This is the formula for a penny-shaped crack opened under constant opening-mode loading $-\sigma$ (Sneddon and Lowengrub, 1969, p. 139).

If one dimension, say the dip dimension, is much larger than the other (Fig. 5), then $a \gg b$. In relation to b then, in Eq. (2), $a \to \infty$ so that $\varepsilon \to 1$. Using $E(1) = 1$ and the above relation between shear modulus and Young's modulus, from Eq. (3) we obtain:

$$u = \frac{-2\sigma(1-\nu^2)}{E}(b^2 - y^2)^{1/2}. \quad (6)$$

This is the plane-strain formula for a two-dimensional elliptical through crack (a 'tunnel crack', Fig. 5) subject to constant opening-mode loading, $-\sigma$ (e.g. Sneddon and Lowengrub, 1969, p. 29). If the true dip dimension is short (but still assumed infinite), a slightly different plane-stress formula is commonly used (Paris and Sih, 1965; Tada et al., 1973). In Eq. (6), u depends only on the smaller dimension, b, which is thus the controlling dimension.

Commonly, the measured displacement of a fracture is known, or assumed, to be its maximum normal displacement, u_{max}, which occurs at the centre of the crack. Substituting $x = y = 0$ in Eq. (3), with the above relation between Young's modulus and shear modulus, we get:

$$u_{max} = \frac{-2\sigma(1-\nu^2)b}{EE(\varepsilon)} \quad (7)$$

which shows that the maximum displacement depends primarily on the smaller dimension b. The only effect of the larger dimension, a, is through the eccentricity, ε, and the value of $E(\varepsilon)$. For example, if $a = 2b$, we obtain $E(\varepsilon) \cong 1.21$, if $a = 3b$, $E(\varepsilon) \cong 1.11$, and if $a = 4b$, $E(\varepsilon) \cong 1.06$, and less for greater a/b ratios. Thus, for the aspect ratios of interest, $E(\varepsilon)$ is always close to unity and the resulting displacement very similar to that obtained in the centre of a through crack (Eq. (6) with $y = 0$). These conclusions indicate that it is the smaller dimension that has the greatest effect on the displacement of an elliptical crack, particularly when

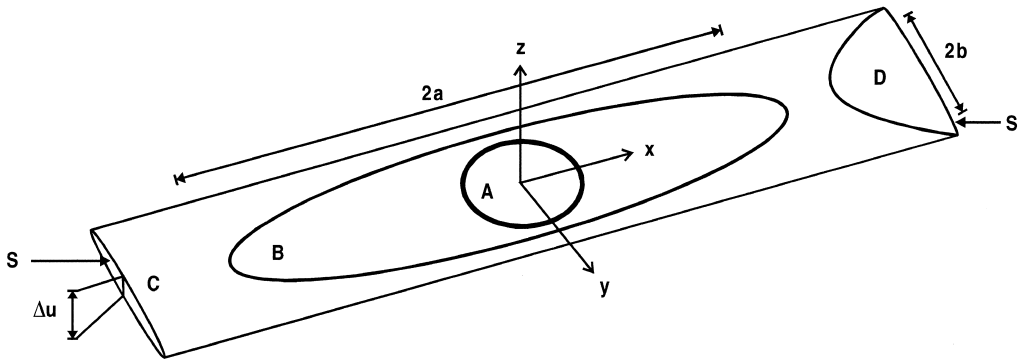

Fig. 5. In relation to the elastic body hosting the crack, ideal, elliptical cracks can have three basic shapes: (A) and (B) an interior crack, (C) a through crack, and (D) a part-through crack. The circular interior crack (A) is a special case of the general, three-dimensional elliptical interior crack (B) with a major axis $2a$ and a minor axis $2b$. The through crack (C), here a long 'tunnel crack', extends from one free surface (S) to another (S) where its maximum opening displacement is Δu. The part-through crack (D) extends from one free surface (S) partly into the elastic body. The orientation of the co-ordinate system, hence the strike and dip of the cracks, are arbitrary. Interior cracks (A and B) are non-restricted in their development; the other two shapes (C and D) are restricted.

the a/b ratio is large, and may therefore be regarded as its controlling dimension.

3. Fracture displacements and apertures

The way that the displacement, and slip or opening in individual events, of a fracture depends on its controlling dimension and shape is illustrated by the equations below. In all these equations, E denotes Young's modulus, ν denotes Poisson's ratio, L denotes the strike dimension of the fracture and R its dip dimension. When the strike dimension is much greater than the dip dimension, a plane-stress formulation should be used. Conversely, when the dip dimension is the greater one (Fig. 5), a plane-strain formulation should be used (Paris and Sih, 1965; Tada et al., 1973), as in Eqs. (5)–(7).

Consider an extension fracture that goes through the elastic layer hosting it. This configuration may apply, for example, to a vertical extension fracture reaching from the surface of a young pahoehoe basaltic lava flow (Fig. 6) to a horizontal, open contact between the flow units (Fig. 7). If a shallow flow unit, or a group of units, is largely decoupled from the underlying units by a well-open contact (a discontinuity), the rock may behave similarly to that of a solid plate with free surfaces at its bottom and top. The extension fracture can then be modelled as a through-the-thickness mode I crack (Fig. 5). From Eq. (7) it follows that if $a > 2$–$3b$, we may use Eq. (6) to calculate approximately the displacement in the centre of the crack. Thus if the strike dimension $L = 2b$ is much smaller than the dip dimen-

Fig. 6. Small extension (tension) fracture initiating from columnar (cooling) joints at the surface of a Holocene pahoehoe lava flow in that part of the rift zone of North Iceland shown in Fig. 1. The length of the fracture is 75 cm, and its greatest opening is 5 cm. As the fracture propagates down through the flow units of the host rock (Fig. 7), its geometry alternates between a part-through crack (when its lower end is inside a flow unit) and a through crack (when its lower end is at an open, freely slipping contact). For unequal rates of vertical and horizontal propagation, the fracture controlling dimension alternates between the strike and dip dimensions.

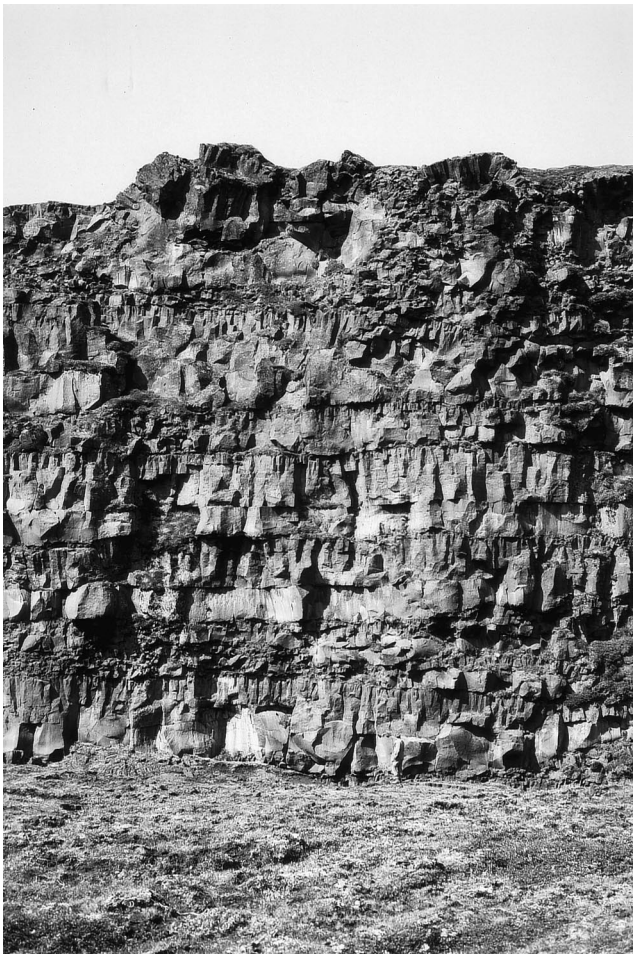

Fig. 7. Cross-section showing the uppermost part of a Holocene pahoehoe lava flow in the rift zone of North Iceland (cf. Fig. 6). View west, this cross-section is part of the footwall of a normal fault with a displacement of around 20 m (the height of the wall). Most flow units range in thickness between 1–3 m and develop regular systems of vertical columnar (cooling) joints. Many flow units have sharp, open contacts that, when subject to tectonic stresses, may be essentially freely slipping near the surface.

sion $R=2a$ (Fig. 5), the associated aperture or opening displacement Δu_{I} depends on the strike dimension. With $y = 0$, Eq. (6) then gives:

$$\Delta u_{\mathrm{I}} = \frac{-2\sigma(1-\nu^2)L}{E}. \tag{8}$$

If, however, the extension fracture goes only partly into the layer hosting it (Fig. 5) and its strike dimension is much greater than its dip dimension, say $L > 2$–$3R$, the controlling dimension is the dip dimension R and a plane-stress mode I crack model gives the following equation (Tada et al., 1973):

$$\Delta u_{\mathrm{I}} = \frac{-4\sigma RV}{E} \tag{9}$$

the function $V(\frac{R}{T})$, where T is the total thickness of the rock layer hosting the fracture, being defined (using radians) as:

$$V\left(\frac{R}{T}\right) = \frac{1.46 + 3.42\left[1-\cos\left(\pi R/2T\right)\right]}{\left[\cos\left(\pi R/2T\right)\right]^2}. \tag{10}$$

For faults, the driving shear stress $\Delta\tau$ is the difference between the remote applied shear stress, τ, and the residual frictional strength on the fault after sliding (Nur, 1974; Rice, 1980). The residual frictional strength is then considered equal to the coefficient of sliding friction multiplied by the normal stress, that is, the term $\mu\sigma_n$ in the Modified Griffith Criterion (Jaeger and Cook, 1969; Nur, 1974), and, denoting the host-rock tensile strength by T_0, we get:

$$\tau = 2T_0 + \mu\sigma_n. \tag{11}$$

A large strike-slip fault is normally modelled as a mode III crack (e.g. Pollard and Segall, 1987), where the displacement Δu_{III} is related to the dip dimension R of the fault according to the equation:

$$\Delta u_{\mathrm{III}} = \frac{4\Delta\tau(1+\nu)R}{E}. \tag{12}$$

For a dip-slip fault where the strike dimension L controls the displacement, a mode III crack is the appropriate model, thus:

$$\Delta u_{\mathrm{III}} = \frac{2\Delta\tau(1+\nu)L}{E}. \tag{13}$$

Conversely, for a dip-slip fault where the dip dimension R controls the displacement, a mode II crack is the appropriate model and is given by:

$$\Delta u_{\mathrm{II}} = \frac{4\Delta\tau RV}{E}. \tag{14}$$

4. Extension fractures and normal faults

To see what effect different controlling dimensions can have on the resulting displacements, one must first consider what are the likely shapes of rock fractures. Nicol et al. (1996) studied the dip dimensions vs. strike dimensions of 40 main-shock slip-surfaces, as defined by aftershock loci, for various types of faults associated with M4.2–6.8 events (Fig. 8). These results, as well as studies of subsurface faults in mining areas (Rippon, 1985; Nicol et al., 1996), suggest that for moderate to large faults the controlling dimension can be either the dip or (less commonly) the strike dimension. There is also a significant difference in the resulting displacement depending on whether the fracture is a through crack or part-through crack. This difference in geometry is illustrated in Fig. 5, and the differences in displacements follow from Eqs. (8)–(10).

Consider an extension fracture that is 200 m long (Fig. 2) and 500 m deep. Assume that at its bottom the fracture meets with a freely slipping horizontal discontinuity, such as a joint, an open contact (Fig. 7) or a very soft sediment, so that the through-crack model is appropriate. The static Young's modulus of the uppermost few hundred metres of the rift zone in Iceland is about 5 GPa, its Poisson's ratio is 0.25, and the in-situ tensile strength of the crust is around 4 MPa (Gudmundsson, 1988). Substituting these values for the dimensions and elastic constants in Eq. (8), and taking the tensile stress at fracture formation to

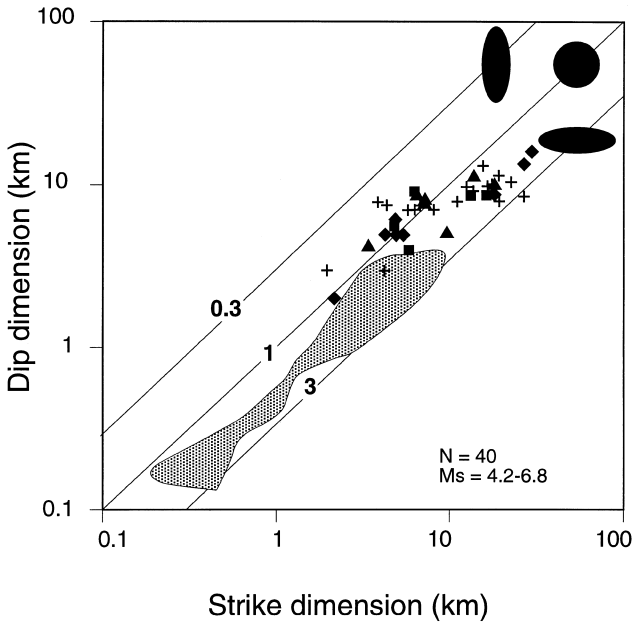

Fig. 8. Dip dimensions plotted against strike dimensions of 40 main-shock slip-surfaces (data from Nicol et al. 1996). The geometries of the main-shock surfaces are defined by the aftershock loci for normal (squares), strike-slip (crosses), reverse (diamonds) and oblique-slip (triangles) faults.

be equal to the in situ tensile strength, the calculated opening displacement is 0.3 m.

If the 200 m long fracture was much shallower, however, the relation between length and displacement would be very different. If the strike dimension is again 200 m, but the dip dimension is 100 m, the ratio of these dimensions, 2.0, is similar to the most common ratio found by Nicol et al. (1996). Let the fracture be a part-through crack in a layer of thickness 500 m. Then the factor T in Eq. (10) is 500 m, whereas the factor R is 100 m, and $V(\frac{R}{T})$ gives a value of approximately 1.8. Substituting this value in Eq. (9), and using the same elastic constants and tensile stress as before, the calculated opening displacement is roughly 0.6 m; twice as large as in the previous case.

These results show that for the same length of extension fracture, in a single tectonic regime with the same elastic constants and tensile stress, the resulting opening displacement depends strongly on the controlling dimension of the fracture and whether or not the fracture is a through-going crack. For fractures of the same length, a shallow fracture would have a wider opening at the surface than a deep fracture. This indicates that a large scatter in a plot of lengths of extension fractures against their widths (Fig. 3) may be partly the result of different fracture geometries and controlling dimensions within the data set.

Fig. 9. Water-filled extension fracture in the Holocene pahoehoe lava flow of the Thingvellir Fissure Swarm in Southwest Iceland (Fig. 2). Although fluid pressure may contribute to their formation, normal faults and extension fractures in rift zones are primarily generated by shear and tensile stresses associated with the divergent plate movements. View northeast, this extension fracture is as wide as 10 m and filled with groundwater to a depth of tens of metres (cf. Gudmundsson 1987b).

Consider now the effects of controlling dimensions on the displacements and slips on normal faults. Many large normal faults in the rift zone of Iceland are around 6 km long (Gudmundsson, 1987a,b). For a strike dimension of 6 km, and a ratio of 2.0 between the strike dimension and the dip dimension (Nicol et al., 1996), the dip dimension would be 3 km and, therefore, the controlling dimension. For the uppermost 3 km of the rift zone in Iceland, the static Young's modulus is around 22 GPa and Poisson's ratio around 0.25. The total thickness of the seismogenic crust in the rift zone of Iceland is commonly around 12 km, in which case the R/T ratio in Eq. (10) is 1/4 and the value of $V(\frac{R}{T})$ about 2.0. Substituting these values in Eq. (14), and using the average driving stress of 3 MPa (Nur, 1974; Kasahara, 1981; Scholz, 1990), one obtains a displacement of just over 3 m.

A different displacement would be obtained on the above normal fault if it extended to the bottom of the seismogenic layer at 12 km depth. In that case the strike dimension of 6 km would be the controlling dimension, and the average static Young's modulus of the whole crust, 40–50 MPa (Gudmundsson, 1988), should be used. Using a Poisson's ratio of 0.25 and a driving stress of 3 MPa, from Eq. (13) one obtains a displacement of around 1 m. Thus, depending on the controlling dimension (here also affecting the value of Young's modulus), the slip on a normal fault with the same driving stress can easily vary by a factor of 3.

5. Fluid transport in extension fractures

Consider a fluid-filled extension (mode I) fracture (Fig. 9) with a strike dimension L smaller than its dip dimension R. If the fracture is a through crack, it follows from Eq. (8) that its aperture or opening displacement Δu_{I} is related to the overpressure Δp of the fluid through the equation:

$$\Delta u_{\mathrm{I}} = \frac{2\Delta p(1-\nu^2)L}{E} \tag{15}$$

where, as before, E is Young's modulus of the rock and ν its Poisson's ratio. If, however, the fluid-filled extension fracture is a part-through crack and its strike

dimension L is greater than its dip dimension R, the controlling dimension is R and, from Eq. (9), the fracture aperture is given by:

$$\Delta u_{\mathrm{I}} = \frac{4\Delta pVR}{E}. \tag{16}$$

Eqs. (15) and (16) show that fluid overpressure can have great effects on the aperture of fluid-conducting fractures.

To see the effects that changes in fracture aperture have on fluid transmission through fractures, consider first the hydraulic conductivity of a single crack, K_{c}, which is given by:

$$K_{\mathrm{c}} = \frac{\rho g \Delta u_{\mathrm{I}}^2}{12\mu} \tag{17}$$

where ρ is the density of the fluid, g is the acceleration due to gravity, Δu_{I} is the crack aperture and μ is the dynamic (or absolute) viscosity of the fluid. Similarly, the volumetric rate of fluid Q_{c} through a crack of unit controlling (smaller) dimension is:

$$Q_{\mathrm{c}} = \frac{\rho g \Delta u_{\mathrm{I}}^3}{12\mu} \nabla h \tag{18}$$

where ∇h is the hydraulic gradient. Eqs. (17) and (18) indicate how sensitive the hydraulic conductivity and associated volumetric flow rates are to changes in fracture aperture. These equations are for individual fractures, but are easily extended to fracture sets (Bear, 1993; Lee and Farmer, 1993) such as those in the damage zones of major fault zones. Thus, when subject to fluid overpressure, the fault-zone hydraulic conductivity and transmissivity can greatly increase.

In order to evaluate the effects of aperture range on fluid transport in rock fractures, we shall consider the results of the measurements of several hundred mineral-filled veins of a major fault zone in North Iceland (Gudmundsson, 1995, 1999). The veins are mostly filled with quartz, chalcedony and zeolites and occur in sets within the damage zone of the fault zone. Some veins occupy shear fractures, but the great majority are pure extension (mode I) cracks (Gudmundsson, 1999). Because the veins occur in sets, many of them are restricted, that is, end in other veins, rock discontinuities or free surfaces.

Several hundred non-restrictive (as seen in the outcrop), extensional mineral veins were selected for studying the width/length ratios (Gudmundsson, 1999). The results (Fig. 10) show a large scatter in the data, similar to the scatter in Figs. 3 and 4. Thus, the width of a mineral vein of a given length can vary by a factor of up to 20 or more, although most commonly the variation is by a factor of roughly 2–10.

If the width or aperture of a mineral vein in a set can vary by a factor of 2, it follows from Eq. (18) that, other things being equal, the volumetric rate of flow through fractures of that given length (smaller dimension) can vary by a factor of 8. If a fracture of a given length exceeds the average width (aperture) of fractures of that length by a factor of 10, the volumetric flow through that single fracture, other things being equal, would be as much as 1000 times that through the fracture of average width. In other words,

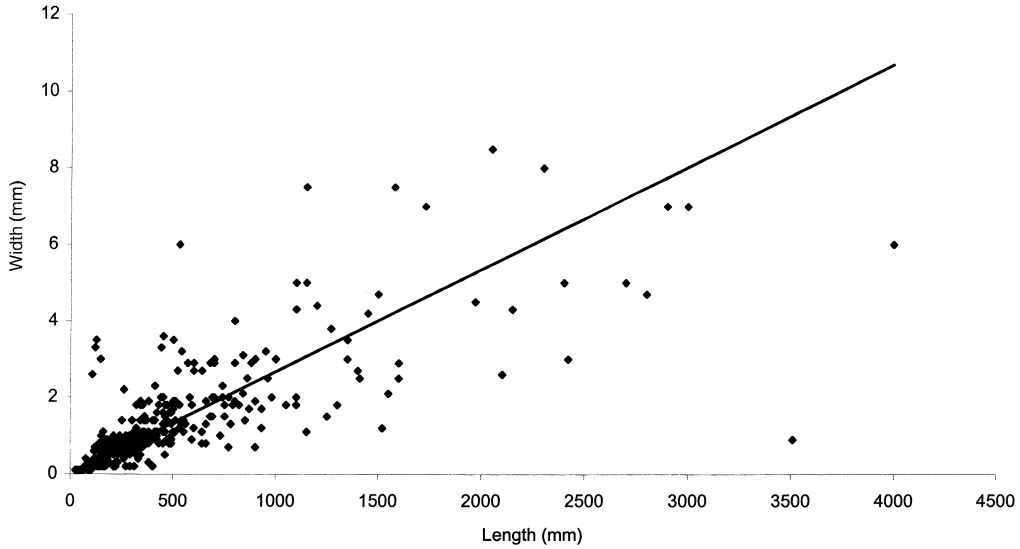

Fig. 10. Length–width (thickness) relationship for 384 mineral-filled veins in the Tjornes Fracture Zone in North Iceland (cf. Gudmundsson, 1995, 1999). All the veins are measured in roughly 12 Ma basaltic lava flows with similar mechanical properties. The regression line indicates that the general length/width ratio is around 400. The linear correlation coefficient $R = 0.81$. There is large scatter in the data: for many veins of the same length, the width varies by a factor of 2–10, and, for some of the smallest veins, the variation is by up to a factor of 20.

a single wide fracture in a set containing hundreds of fractures can largely control the fluid flow through that set. It follows that any realistic model on fluid flow in rock fractures must take into account the effects of controlling dimensions on fracture apertures and the way these parameters change during the evolution of the fluid-transporting fracture system.

6. Discussion

Most fractures grow by segment linkage (e.g. Gudmundsson, 1987a,b; Willemse et al., 1996), which has also been suggested as a possible explanation for scatter in the length-displacement data (Cartwright et al., 1995). The results presented in this paper indicate that different controlling dimensions of fractures may largely explain this scatter. Furthermore, when a fracture grows by segment linkage its controlling dimension is likely to change. For example, a normal fault may start its growth when a set of extension fractures link up, as is commonly observed in the field (Pollard et al., 1982; Gudmundsson, 1987a,b; Willemse et al., 1996). The controlling dimension of each of the extension fractures may be the strike dimension, but when they link up during their lateral propagation, the dip dimension may become the smaller, and thus the controlling, dimension. If this normal fault eventually propagates through the whole crust, which in a rift zone is underlain by magma (Gudmundsson, 1988), the strike dimension again becomes the controlling dimension.

Similar changes in controlling dimensions may occur for fractures at any scale, particularly those that are growing in a layered rock (Figs. 6 and 7). Field measurements (Amadei and Stephansson, 1997) and theoretical studies (Bonafede and Rivalta, 1999) indicate that abrupt changes in the stress field controlling the fracture growth are common at contacts and other discontinuities in a stratified rock. Fractures that meet with these discontinuities may act as through cracks while stopping at the contacts, but later when they have propagated through the contacts, they act as part-through cracks.

Changes in controlling dimensions of fractures constituting fluid-transporting networks (e.g. Sibson, 1996) may have great temporal effects on the overall fluid transmissivity of the network. Fractures of a given length, and constituting networks located in a single tectonic regime with essentially uniform mechanical host-rock properties, commonly have apertures that differ in size by a factor of up to 10. Such a large scatter is likely to be partly due to the fracture apertures being related to different controlling dimensions. For some fractures in the network, the aperture is a function of the strike dimension, whereas for others the aperture is a function of the dip dimension. During the evolution of the network, the controlling dimensions may alternate between the dip and the strike dimensions.

While moderate to large faults are commonly slightly elongate in the strike dimension (Fig. 8), many rock fractures may be elongate in the dip dimension. For example, small extension fractures in basaltic lava flow (Fig. 6) propagate through linking up of vertical columnar joints through horizontal contacts between flow units (Fig. 7; cf. Gudmundsson, 1992). Such fractures are likely to change their controlling dimensions many times during their evolution into large normal faults (Figs. 1–4). The dimensions of a given rock fracture depend on variations in tensile strength, Young's modulus and stresses in the rock hosting the fracture and, for hydrofractures (Fig. 10), on fluid pressure gradients in the fracture. The resulting dip dimension may thus be greater than the strike dimension.

It is well known that fluid flow in fractured media differs from that in porous media in that the hydrogeological properties of the fractured media are much more sensitive than those of the porous media to changes in the associated stress field. This difference has mainly been attributed to the apertures of the fractures changing much more easily when the stress field changes than the near-spherical voids of the porous media. The considerations in this paper, however, indicate that not only are the fractures, and associated permeabilities, sensitive to changes in the stress field, but also to changes in the controlling dimensions of the fractures. It follows that realistic models applied to fluid flow in rock fractures should take into account the controlling dimensions and the way they may change during the evolution of the fracture system.

Acknowledgements

The work reported here was initiated while I was a visiting professor at the Université Pierre et Marie Curie in Paris, where Jacques Angelier, Francoise Bergerat and Daniel Mege made my stay pleasant and fruitful. I thank Maurizio Bonafede, Joe Cartwright, Noelle Odling and Richard Schultz for helpful comments; Hallstein Lie and Kellfrid Lyslo for help with Figs. 5 and 10, respectively; and the European Commission (through contracts ENV4-CT96-0252 and EVR1-CT-1999-40002) and the Research Council of Norway for financial support.

References

Amadei, B., Stephansson, O., 1997. Rock Stress and its Measurement. Chapman & Hall, New York.

Bear, J., 1993. Modelling flow and contaminant transport in fractured rocks. In: Bear, J., Tsang, C.F., Marsily, G. (Eds.), Flow and Contaminant Transport in Fractured Rock. Academic Press, New York, pp. 1–37.

Beyer, W.H., 1976. Standard Mathematical Tables, 24th edition. CRC Press, Cleveland, Ohio.

Bonafede, M., Rivalta, E., 1999. On tensile cracks close to and across the interface between two welded elastic half-spaces. Geophysical Journal International 138, 410–434.

Broberg, K.B., 1999. Cracks and Fracture. Academic Press, London.

Cartwright, J.A., Trudgill, B.D., Mansfield, C.S., 1995. Fault growth by segment linkage: an explanation for scatter in maximum displacement and trace length data from the Canyonlands Grabens of SE Utah. Journal of Structural Geology 17, 1319–1326.

Clark, R.M., Cox, S.J.D., 1996. A modern regression approach to determining fault displacement–length scaling relationships. Journal of Structural Geology 18, 147–152.

Cowie, P.A., Scholz, C.H., 1992. Displacement–length scaling relationships for faults: Data synthesis and discussion. Journal of Structural Geology 14, 1149–1156.

Cowie, P.A., Knipe, R.J., Main, I.G., 1996. Introduction to the Special Issue. Journal of Structural Geology 18, v–xi.

Dawers, N.H., Anders, M.H., Scholz, C.H., 1993. Growth of normal faults: displacement–length scaling. Geology 21, 1107–1110.

Green, A.E., Sneddon, I.N., 1950. The distribution of stress in the neighbourhood of a flat elliptical crack in an elastic body. Proceedings of the Cambridge Philosophical Society 46, 159–163.

Gudmundsson, A., 1987a. Geometry, formation and development of tectonic fractures on the Reykjanes Peninsula, southwest Iceland. Tectonophysics 139, 295–308.

Gudmundsson, A., 1987b. Tectonics of the Thingvellir fissure swarm, SW Iceland. Journal of Structural Geology 9, 61–69.

Gudmundsson, A., 1988. Effect of tensile stress concentration around magma chambers on intrusion and extrusion frequencies. Journal of Volcanology and Geothermal Research 35, 179–194.

Gudmundsson, A., 1992. Formation and growth of normal faults at the divergent plate boundary in Iceland. Terra Nova 4, 464–471.

Gudmundsson, A., 1995. Stress fields associated with oceanic transform faults. Earth and Planetary Science Letters 136, 603–614.

Gudmundsson, A., 1999. Fluid overpressure and stress drop in fault zones. Geophysical Research Letters 26, 115–118.

Jaeger, J.C., Cook, N.G.W., 1969. Fundamentals of Rock Mechanics. Chapman and Hall, New York.

Kasahara, K., 1981. Earthquake Mechanics. Cambridge University Press, New York.

Kassir, M., Sih, G.C., 1966. Three-dimensional stress distribution around an elliptical crack under arbitrary loadings. Journal of Applied Mechanics 33, 601–611.

Kassir, M., Sih, G.C., 1975. Three-dimensional Crack Problems. Noordhoff, Leyden.

Lee, M.K., Farmer, I., 1993. Fluid Flow in Discontinuous Rocks. Chapman and Hall, London.

Marrett, R., 1996. Aggregate properties of fracture populations. Journal of Structural Geology 18, 169–178.

Nicol, A., Watterson, J., Walsh, J.J., Childs, C., 1996. The shapes, major axis orientations and displacement pattern of fault surfaces. Journal of Structural Geology 18, 235–248.

Nur, A., 1974. Tectonophysics: the study of relations between deformation and forces in the earth. In: Advances in Rock Mechanics, 1 Part A. US National Committee for Rock Mechanics, National Academy of Sciences, Washington DC, pp. 243–317.

Odling, N.E., 1997. Scaling and connectivity of joint systems in sandstones from western Norway. Journal of Structural Geology 19, 1257–1271.

Paris, P.C., Sih, G.C., 1965. Stress analysis of cracks. In: Fracture Toughness Testing and its Application. American Society for Testing of Materials, Philadelphia, pp. 30–81.

Pollard, D.D., Segall, P., Delaney, P.T., 1982. Formation and interpretation of dilatant echelon cracks. Geological Society of America Bulletin 93, 1291–1303.

Pollard, D.D., Segall, P., 1987. Theoretical displacements and stresses near fractures in rock: with applications to faults, joints, veins, dikes and solution surfaces. In: Atkinson, B. (Ed.), Fracture Mechanics of Rock. Academic Press, London, pp. 277–349.

Rice, J.R., 1980. The mechanics of earthquake rupture. In: Dziewonski, A.M., Boschi, E. (Eds.), Physics of the Earth's Interior. North Holland, Amsterdam, pp. 555–649.

Rippon, J.H., 1985. Contoured patterns of the throw and hade of normal faults in the Coal Measures (Westphalian) of north-east Derbyshire. Proceedings of the Yorkshire Geological Society 45, 147–161.

Schlische, R.W., Young, S.S., Ackermann, R.V., Gupta, A., 1996. Geometry and scaling relations of a population of very small rift-related normal faults. Geology 24, 683–686.

Scholz, C.H., 1990. The Mechanics of Earthquakes and Faulting. Cambridge University Press, New York.

Schultz, R.A., 1997. Displacement–length scaling for terrestrial and Martian faults: Implications for Valles Marineris and shallow planetary grabens. Journal of Geophysical Research 102, 12009–12015.

Sibson, R.H., 1996. Structural permeability of fluid-driven fault-fracture meshes. Journal of Structural Geology 18, 1031–1042.

Sih, G.C., Liebowitz, H., 1968. Mathematical theories of brittle fracture. In: Liebowitz, H. (Ed.), Fracture: An Advanced Treatise, 2. Academic Press, New York, pp. 67–190.

Sneddon, I.N., Lowengrub, M., 1969. Crack Problems in the Classical Theory of Elasticity. John Wiley, New York.

Tada, H., Paris, P.C., Irwin, G.R., 1973. The Stress Analysis of Cracks Handbook. Del Research Corporation, Hellertown (Pennsylvania).

Tsang, C.F., Neretnieks, I., 1998. Flow channeling in heterogeneous fractured rocks. Reviews of Geophysics 36, 275–298.

Vermilye, J.M., Scholz, C.H., 1995. Relation between vein length and aperture. Journal of Structural Geology 17, 423–434.

Willemse, E.J.M., Pollard, D.D., Aydin, A., 1996. Three-dimensional analysis of slip distributions on normal fault arrays with consequences for fault scaling. Journal of Structural Geology 18, 295–309.